lubricants

MDPI

The Friction Reducing Effect of Square-Shaped Surface Textures under Lubricated Line-Contacts—An Experimental Study

Ping Lu [1],*, Robert J. K. Wood [1], Mark G. Gee [2], Ling Wang [1] and Wilhelm Pfleging [3]

[1]   National Centre for Advanced Tribology, University of Southampton, SO17 1BJ, Southampton, UK;
     r.wood@soton.ac.uk (R.J.K.W.); ling.wang@soton.ac.uk (L.W.)
[2]   National Physical Laboratory, TW11 0LW, Teddington, UK; mark.gee@npl.co.uk
[3]   Karlsruhe Institute of Technology, Karlsruhe Nano Micro Facility, Hermann-von-Helmholtz-Platz 1,
     76344 Egg.-Leopoldshafen, Germany; wilhelm.pfleging@kit.edu
*   Correspondence: pl1g11@soton.ac.uk; Tel.: +44-772-4709-480

Abstract: Surface texturing has been shown to be an effective modification approach for improving tribological performance. This study examined the friction reduction effect generated by square dimples of different sizes and geometries. Dimples were fabricated on the surface of ASP2023 steel plates using femtosecond laser-assisted surface texturing techniques, and reciprocating sliding line contact tests were carried out on a Plint TE77 tribometer using a smooth 52100 bearing steel roller and textured ASP2023 steel plates. The tribological characterization of the friction properties indicated that the textured samples had significantly lowered the friction coefficient in both boundary (15% improvement) and mixed lubrication regimes (13% improvement). Moreover, the high data sampling rate results indicated that the dimples work as lubricant reservoirs in the boundary lubrication regime.

Keywords: square dimples; laser surface texturing; reciprocating sliding; mixed lubrication

1. Introduction

Surface texturing is an approach to the modification of surfaces to form regular patterns on surfaces. In recent decades, many researchers have reported that surface texturing can contribute to friction reduction at sliding contact interfaces [1,2]. Therefore, surface texturing has been used to improve tribological performance, especially to reduce friction in mechanical components, such as thrust bearings [3], journal bearings [4], piston rings [5], mechanical seals [6], and bio-implants [7].

The earliest research on micro-texturing was presented by Hamilton and co-workers in the 1960s [8]. They illustrated that micro-irregularities are able to generate additional hydrodynamic pressure, so that higher load carrying capacity can be achieved. In 1996, Etsion and Bustein's paper opened a new chapter in this area, and remarkable progress has been made in both theoretical modeling and experimental identification over the past 20 years [9]. In the meantime, research into surface texturing has grown significantly globally by many research groups. From 2002, Wang's group conducted a series of experiments under hydrodynamic to mixed lubrication regimes with water as lubricant, and the results were summarized into a load carrying capacity map, which indicated the influence of the area ratio (the area percentage of the dimples to the total area), and the dimple depth-to-diameter ratio [10]. Apart from circular dimples, various other dimple shapes have also been studied. In 2011, a series of experiments were conducted by Qiu to examine the performance of laser surface textured circular and elliptical dimples on stainless steel rings, and it was found

that all the dimpled specimens helped to reduce the coefficient of friction [11]. In particular, the elliptically-shaped dimple with the long axis aligned in the direction of relative motion between the two surfaces performed better than the other elliptical or circular dimples. In the same year, another reciprocating friction test was conducted by Yu to evaluate the friction reduction effect generated with circular, elliptical, and square dimples [12]. Different from Qiu's results, Yu found the elliptical dimples with the short axis aligned to the sliding direction performed better than the other two shapes. In 2013, a series of triangle-shaped textures were investigated by Wang with different dimple parameters including depth, coverage ratio, size, and direction, and the results showed that the dimple orientation had a great influence on the tribological performance [13]. The dimple orientation's influence was also studied with other shapes. For example, the chevron shaped pattern was studied by Costa [14], Vladescu [15], and Shen [16]. According to their results, the hydrodynamic film thickness was directly influenced by the shape and orientation of the patterns, and the chevron pattern pointing along the sliding direction could increase the hydrodynamic film thickness and build up hydrodynamic pressure efficiently. In conclusion, by reviewing the most relevant experimental results in this area, it can be seen that the effect of texturing on friction depends on both the operating conditions and lubrication regime [17]. It has been reported that wear debris can be trapped in the dimples, thus reducing the third-body wear. Additionally, the textures may work as micro-reservoir for lubricant in lubricant starvation conditions. Furthermore, additional hydrodynamic lift generated by the cavitation effect between contact surfaces helps to reduce the coefficients of friction [18]. In addition, the dimple shape influenced the film thickness and the coefficients of friction significantly, for symmetric shapes, the square dimples performed better than circular shape dimples, since it may have a larger converging wedge than the circular one [12].

Although beneficial effects of using textures to reduce friction have been reported, there is a need for further investigation into the behavior under mixed and boundary lubrication regimes. The aim of the present study is to study experimentally the size influence of square dimples in these lubrication regimes. The friction results were characterized in Stribeck curve form to illustrate the lubricated contact performance.

2. Experimental Details

2.1. The Test Rig

All the tribological tests were conducted on a Plint TE77 reciprocating tribometer (Phoenix Tribology Ltd., Kingsclere, UK). As shown in Figure 1a, a test roller moves in a pure sliding motion against a smooth or textured plate. A pure sinusoidal reciprocating motion was used. This machine has the capability to provide a normal load of up to 1000 N, as well as a sliding frequency of up to 50 Hz. The friction between the roller and the plate is monitored using a piezoelectric transducer and the average friction force was recorded in real time at a data acquisition rate of 1 Hz during the test. In addition, complete friction loops were acquired every 2 min at a much higher sampling rate of 20 kHz.

2.2. Materials and Test Sample Preparation

AISI 52100 cylindrical rollers and ASP 2023 plate specimens were used as the friction pairs. The dimensions of the rollers were φ6 mm × 10 mm, and both ends of the roller have a fillet. The cylindrical surface is smooth with a surface roughness R_a = 0.03 μm. The dimensions of the plate specimens were 60 mm × 22 mm × 4 mm. The roughness of functional surface was about 0.01 μm before texturing. The physical properties of both specimen materials are listed in Table 1.

(**a**)   (**b**)
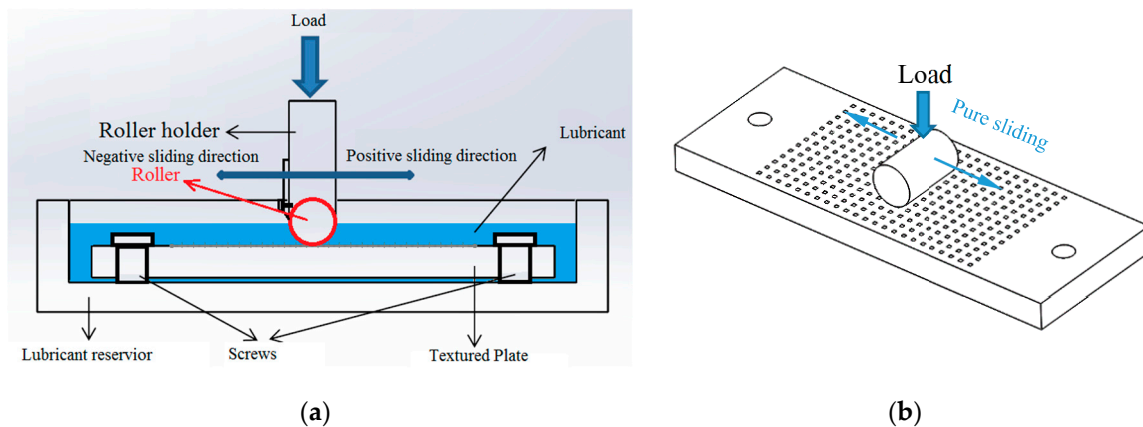
Figure 1. A schematic of (**a**) the TE77 test rig and (**b**) the line contact.

Table 1. Physical properties of friction pairs.

Grade	Density	Elastic Modulus	Hardness	Poisson Ratio
	Kg/m^3	GPa	Vickers hardness (HV)	
Smooth surface material: AISI 52100	7810	200	848	0.28
Textured surface material: ASP 2023	8000	230	800	0.29

Texturing was carried out by Karlsruhe Nano Micro Facility by using a micromachining workstation (PS450-TO, Optec, Frameries, Belgium, Figure 2b) equipped with an ultrafast fiber laser (Tangerine, Amplitude Systèmes, Pessac, France) operating with an average power of 20 W and a maximum pulse energy of 100 µJ at 1030 nm (TEM$_{OO}$ with M^2 < 1.3). By using this special configured workstation (e.g., fundamental and 2nd and 3rd harmonics, tunable pulse length, etc.), complex and high-speed laser micro- and nano-structuring of multi-material systems is possible without inducing thermal impact [19]. High repeatability and reproducibility is also achieved. The pulse duration can be tuned in the range from 350 fs up to 10 ps.

(**a**)   (**b**)
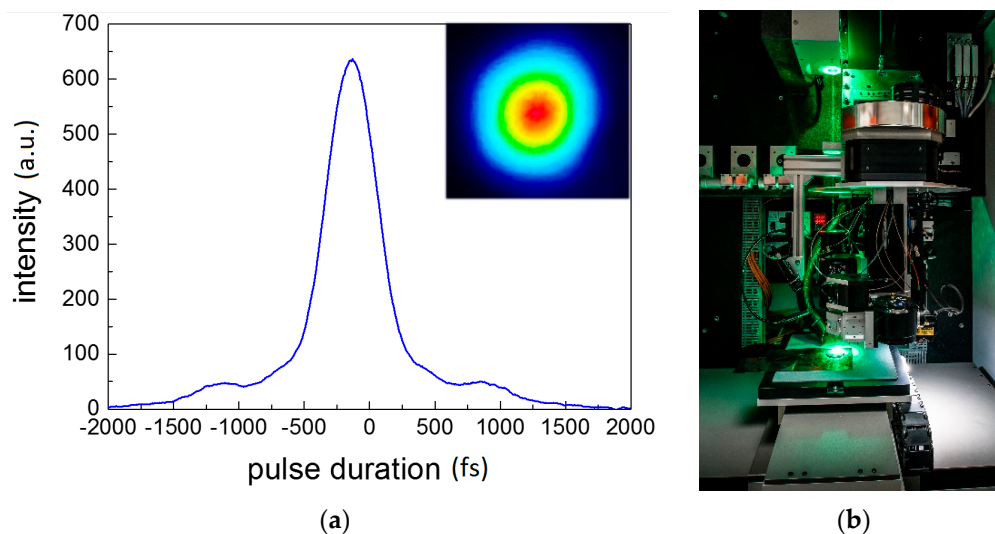
Figure 2. (**a**) Intensity of the laser pulse as function of time (pulse length 350 fs) and Gaussian intensity distribution; (**b**) multi-wavelength ultrafast laser micromachining workstation with a novel Turret Optics design to deploy and index the system's three galvo heads with near-perfect sub-micron repeatability.

The laser structuring of the dimples used in this study was performed using a laser wavelength of 515 nm, a repetition rate of 200 kHz at a laser scanning speed of 200 mm/s. The pulse duration was set to 350 fs (Figure 2a). The laser beam was scanned over the sample surface using a RhothorTM Laser Deflection Systems scan head (Newson Engineering BV, Overmere, Belgium). The process was performed scanning the laser beam using a f-theta lens with a focal length of 100 mm (Figure 2). A laser processing area of 90 mm × 90 mm was achieved by using the scanner. The structuring process was carried out in ambient air. The ablated material was removed during the structuring process by an external exhaust, which has been positioned directly in front of the sample. The extremely short pulses of ultrafast lasers helped to avoid the formation of melt or a heat affected zone (HAZ) with modified mechanical or chemical properties. The depth of dimples was determined by the average laser power, the laser scanning speed and the number of scanning repetitions. A variety of dimple sizes were created to investigate the effect of the dimple size.

Vitrea 32 mineral base oil from Shell (Shell U.K. Limited, London, UK) was used as the lubricant in the frictional tests, and the properties are listed in Table 2.

Table 2. Properties of Vitrea 32 mineral base oil.

| Density	Kinematic Viscosity	Kinematic Viscosity	Pressure-Viscosity Coefficient
at 15 °C (ρ)	at 40 °C (υ_0)	at 100 °C (υ_1)	(α)
868 kg/m^3	32 mm^2/s	5.4 mm^2/s	12.8×10^{-9} m^2/s

2.3. Experimental Procedures

The tests were conducted under room temperature, which is around 24 °C in a temperature controlled lab. However, due to the heat generated by the friction, the temperature of the oil was stabilized at about 32 ± 1 °C after running in. The selected lubricant under this temperature has the following properties: pressure-viscosity coefficient α = 12.8 × 10^{-9} m^2/N, kinematic viscosity υ = 48 mm^2/s, and the dynamic viscosity η = 0.042 Pa·s. For each test, around 15 mL oil was used to submerge the plate specimen.

The λ ratio was used to define the lubrication regime, and the minimum mid-stroke film thickness was calculated using Dowson and Higginson's equation [20] for line contacts. Additionally, the dimensionless parameter $\eta VL/W$ was used to produce Stribeck curves, where η is the lubricant dynamic viscosity, V is the contact speed, L is the roller length and W is the normal load. The loading conditions were set to be 100 N and 350 N, with the mid-stroke sliding speed ranging from 0.03 to 0.47 m/s. Under these test conditions, the mid-stroke λ ratio ranges from 0.5 to 3.7, while the Stribeck parameter ranges from 3.77 × 10^{-8} to 1.98 × 10^{-6}. Typically, the λ ratio ranges from 1 to 3 in mixed lubrication regime, while $\lambda < 1$ represent for boundary lubrication regime and $\lambda \geqslant 3$ for EHL [21].

The test procedure was designed as follows. Firstly, the lubricated friction tests were started at a constant normal load of 100 N, while the frequency was set in the range from 15 to 1 Hz. In the second step, the normal load increased to 350 N, and the frequency was reset from 15 to 1 Hz again. During experiments, the frequency of sliding was decreased in a stepwise manner with a stroke length of 10 mm. The test duration for each frequency was set to 8 min, except for the 15 Hz condition lasted for 18 min. The friction tests went through from the first step to the last step following the procedure described in Figure 3. In order to verify the reproducibility of results, each test was repeated twice, and each test was completed with a new roller on a new track of the plate surface.

The initial Hertzian line contact pressure and contact width of the contact area under certain loads were calculated by cylinder on plane equations [22], and the results are presented in Table 3.
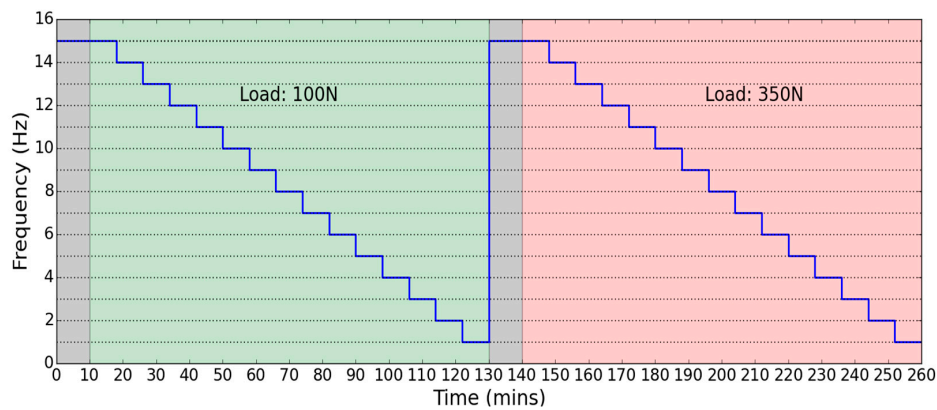
Figure 3. Test procedures.

Table 3. Initial Hertzian line contact pressure for ASP 2023 samples vs. AISI 52100 Roller.

Load (N)	Contact Width (μm)	Mean Contact Pressure (GPa)	Maximum Contact Pressure (GPa)
100 N	36	0.28	0.35
350 N	68	0.52	0.66

Surface topography measurements were taken before every test. The geometrical parameters of the textures on the plate were measured using Alicona Infinite-Focus (Alicona Imagine GmbH, Raaba, Austria), and the roughness was measure by Taylor Hobson Form Talysurf 120L stylus profilometer (Taylor Hobson Ltd., Leicester, UK).

2.4. Sample Parameter

All the dimples in this study were square with flat bottom, as shown in Figure 4. Parameters *a* and *b* are the sizes of dimples, *h* is the depth of the dimple, and l is the length of the unit cell.
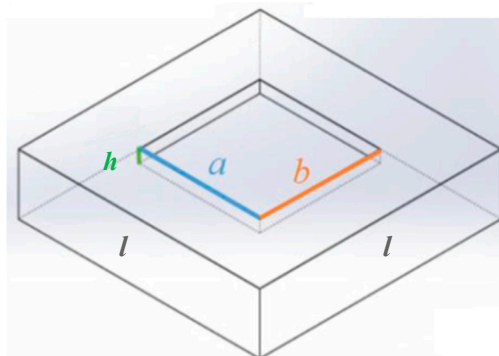
Figure 4. Design schematic of a single dimple.

The dimple coverage ratio is defined as the ratio of the area occupied by the dimple to the imaginary unit cell as follows:

$$cr = \frac{S_D}{S} = \frac{a \cdot b}{l^2} \ (\%) \tag{1}$$

where *cr* is the dimple coverage ratio, S_D is the area occupied by dimple, and *S* is the area of the unit cell.

In this study, the focus is on the friction reduction effect influenced by the dimple size. The design parameters are listed in Table 4. S, M and L represent the small, medium and large dimples, separately.

**Table 4.** Design parameters of S, M and L samples.

Sample	Side Length	Side Length	Maximum Dimple Depth	Interval Length	Area Density
No.	(a/μm)	(b/μm)	(h_D/μm)	(l/μm)	(cr/%)
S	250	250	15	790	10
M	375	375	15	1185	10
L	500	500	15	1580	10

All surfaces were examined using the Alicona prior to reciprocating testing. For each specimen, five dimples were randomly picked and measured to check the surface topography of the dimples, and the average value of these dimples are recorded in Table 5 as the actual parameters.

Table 5. Actual parameters of S, M and L samples.

Sample	Side Length	Side Length	Maximum Dimple Depth	Interval Length	Area Density
No.	(a/μm)	(b/μm)	(h_D/μm)	(l/μm)	(%)
S	240 ± 5	240 ± 5	13 ± 2	790 ± 5	9.1
M	375 ± 5	375 ± 5	8 ± 3	1185 ± 5	10.0
L	480 ± 5	480 ± 5	10 ± 1	1580 ± 5	9.2

The S, M and L profiles are shown in Figure 5. The color maps present the surface topography of a dimple, and the cross-section profiles were obtained in middle of dimples (shown in white dash line).
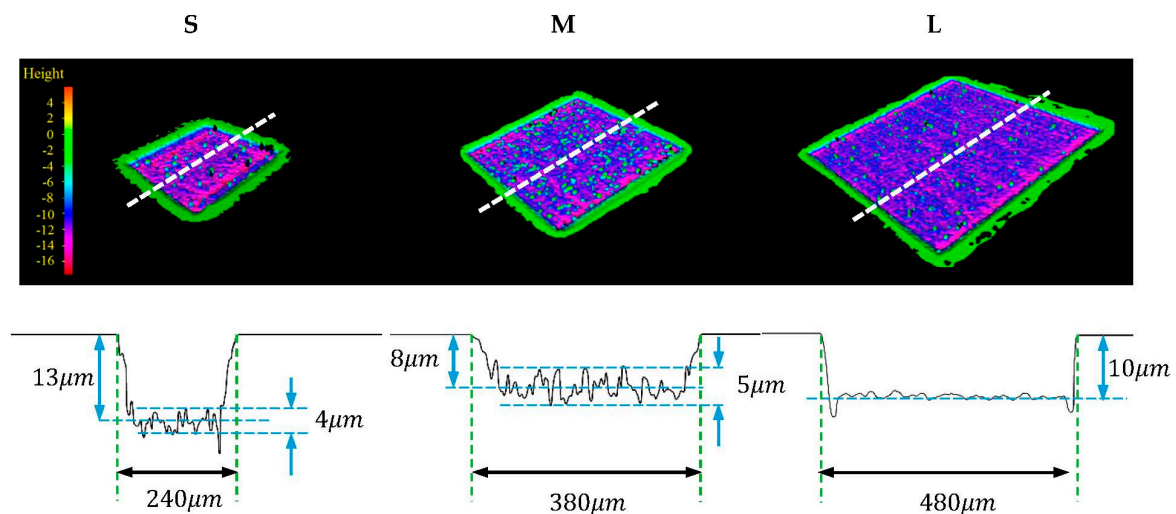

Figure 5. S, M and L dimple profiles.

It can be observed from Figure 5 that the edges of dimples are very smooth; no rims appear owning to the benefit of using ultra-fast laser surface texturing. However, due to the limitation of manufacturing accuracy, the edges of dimples are not perfectly perpendicular to the surfaces, and small angle appears on edges of the cross-section shape. It was also found that all the dimples have round corners instead of square corners, with the radius at corners for all samples less than 30 μm. The bottom of the small and medium sized dimples was quite rough, and the dimple depth was shallower than designed due to manufacturing errors. By comparison, the large dimples had comparable smooth bottoms with an average roughness of less than 1 μm.

3. Results and Discussion

In this section, the results of the reciprocating sliding tests are presented. The dynamic coefficients of friction of the dimpled surfaces are compared with that of the non-textured samples. Additionally, the friction data sampled at the high rate is presented to show the local friction variation caused by dimples.

3.1. Friction Force Stability versus Time

The stability of results was assessed before discussing the test results. Figure 6 shows the friction and displacement versus time responses in one second for the smooth surfaces under the conditions of normal load at 100 N, reciprocating frequency of 10 Hz and oil temperature of 32 °C.
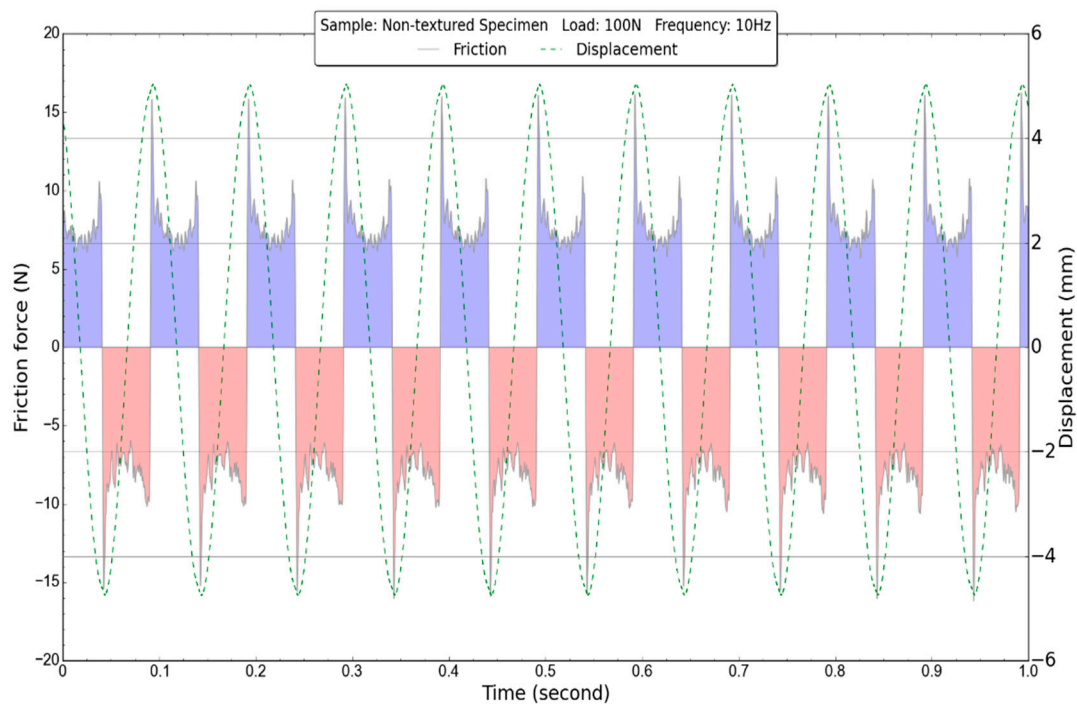

Figure 6. One-second data of non-textured specimen (test conditions: Normal load: 100 N, Frequency: 10 Hz, Oil temperature: 32 °C).

In this figure, the blue part represents the friction force variation against time when the roller pin slides towards the negative direction, as marked in Figure 1a. The pink part shows the friction value on the opposite sliding direction; here the minus sign for the friction force only indicates the friction force direction, instead of a negative value. The green dashed line shows the displacement of the roller, with the position is labeled in the right axis. The analysis of the friction responses show that a small fluctuation of the friction occurred during the first 8 min of the tests, i.e., the running-in period, but stabilized during the rest of the tests. Also, it should be noted that all the tests showed the same level of stability.

3.2. Baseline Results

The coefficient of friction under different load and speed conditions from the baseline tests are summarized in Figure 7. The data used in the Stribeck curve was the average value of 2000 data points from the middle of the stroke (20,000 data points in 1 s).
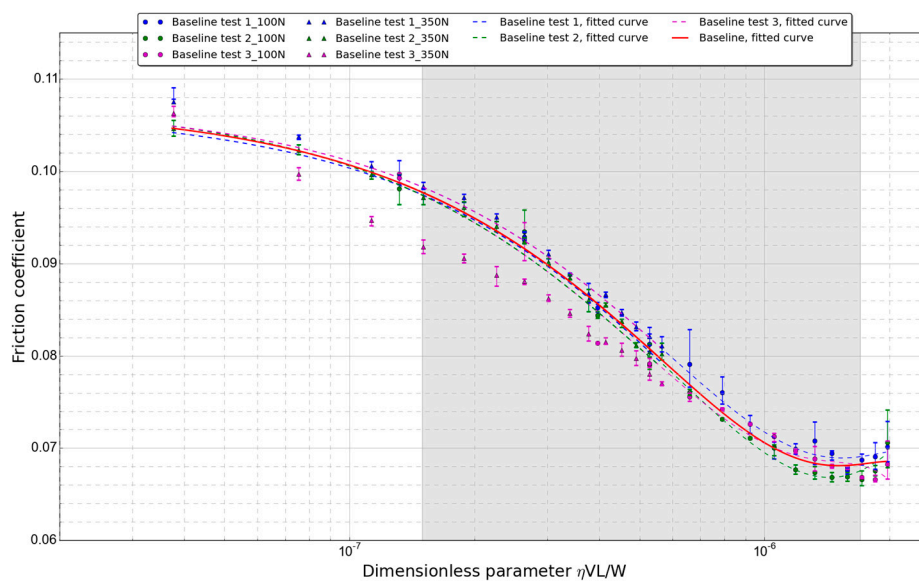
Figure 7. Stribeck curve showing repeatability between different tests for smooth specimen.

The test was repeated three times with non-textured samples as the baselines, and data ending in 01 mean it was recorded from the first test. The error bars give maximum values and minimum values of four sets of high-speed data generated in the same test. The data ending in 02 give the information from the second test, and the error bars give the value difference between four sets of high-speed data obtained in the same test, and the trend curves were obtained from their mean values. The highlighted area represents the mixed lubrication regime according to calculation, while the boundary lubrication regime and hydrodynamic regimes lie to the left and right of the marked area.

Looking at the trend curve, the repeatability of non-textured samples is seen to be quite good. The average baseline data used the mean value of these three tests. The biggest difference in friction coefficient observed between Test 01 and Test 02 was less than 0.003, and the maximum standard deviation was 0.00056, which was obtained under the load of 100 N at the speed of 0.16 m/s (5 Hz), and the standard error of the mean was 0.00028 at that condition. Compared to the results of Test 01 and 02, the friction coefficients of Test 03 at a load of 350 N was slightly lower, and there were some points clearly laying outside of the curve, which may cause by the unavoidable specimen difference.

3.3. Textured Surfaces Results

For textured samples, each test was repeated twice, and the standard error of mean between tests less than 0.0012 at maximum for the textured sample tests. Compared to the textured sample results, the non-textured samples gave more consistent results, with the standard error of mean only 0.00028 at maximum. Overall, the repeatability of the tests is considered acceptable, and the average values of all samples will be used for comparison in this section.

The difference between the textured and smooth samples on the lubrication and friction performance was compared by examining Stribeck curves, as shown in Figure 8. The squares shown next to the fitted curves are relevant to the dimple sizes (for plates with large, medium or small dimples) giving a better visualization.

It can be seen that the fitted curves for all samples (S, M and L) follow the same trend, and a frictional reduction has been achieved compared with the non-textured samples especially in the boundary lubrication regime with the largest reduction of 15%. Although researchers have claimed that surface texturing could only reduce friction when features are smaller than the contact width [23], the reduction in the boundary regime is in agreement with Wakuda's [24], who previously studied the influence of dimple size on frictional properties and suggested dimple's size larger than contact

width is beneficial for friction reduction. The influence of the dimples on friction in the hydrodynamic regime is however found minimal. Furthermore, the size of the dimples has little influence on the friction coefficient. The fact that samples S, M and L show a similar friction coefficient trend may be because the Hertzian contact width between the roller and plate was much smaller than the dimple sizes, and a single dimple was not fully covered by the roller, as shown in Figure 9, which makes it difficult to generate hydrodynamic lift.
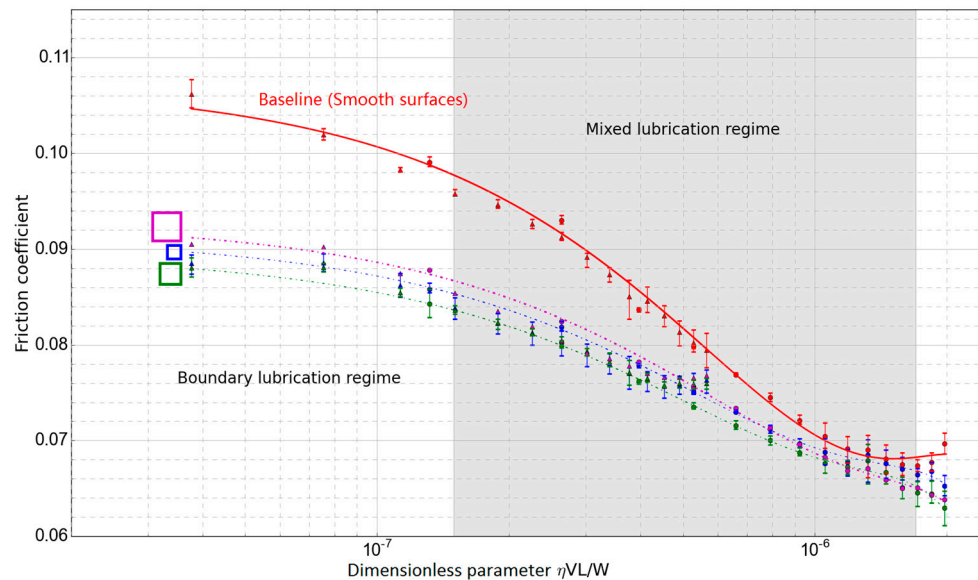
Figure 8. Friction reduction by flat bottom dimples (S: 250 μm × 250 μm × 15 μm, M: 375 μm × 375 μm × 15 μm, L: 500 μm × 500 μm × 15 μm).
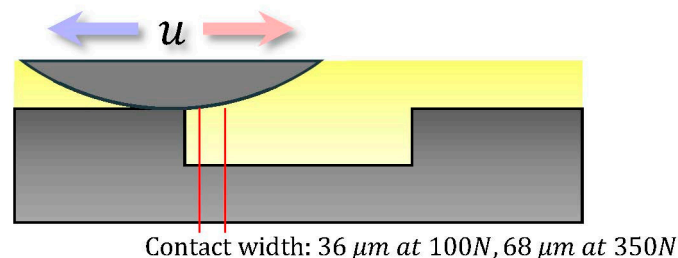
Figure 9. Relationship between contact width of mating elements and dimple size.

To investigate the correlation between friction and dimples, the single stroke friction values sampled at the higher rate were analyzed. Before this, the wear scars on the tested specimen were imaged using Alicona (10×) to locate the dimple array positions, as shown in Figure 10, and the measurement of dimple arrays are listed in Table 6.

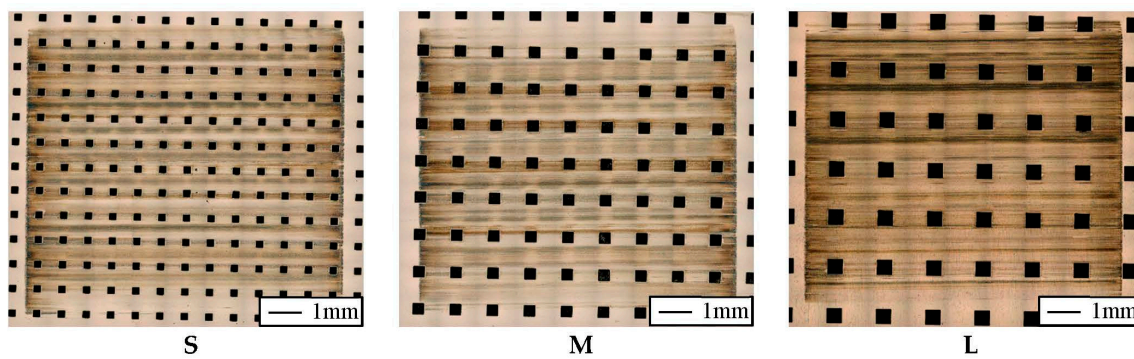**Figure 10.** Wear scar measurement.

Table 6. Measurements of wear scar.

Sample	Dimple Numbers	First Dimple Position (left) (Left Edge)	Wear Scar Length (Horizontal Direction)	Wear Scar Width (Vertical Direction)
No.		(mm)	(μm)	(μm)
S	13	−4.460	10,194	9300
M	9	−4.875	10,178	9055
L	6	−4.100	10,184	9145

For the single stroke data analysis, 4 sets data from each test were averaged and drawn against dimple position in Figure 11. The left column in Figure 11 shows the friction under the low load condition (load: 100 N and frequency: 2 Hz), and the right column presents the results under high load condition (load: 350 N and frequency: 2 Hz). The red solid line represents that the roller sliding towards the positive direction (same with the direction marked in red shown in Figure 9), while the blue solid line shows the opposite situation.

It should be noticed that, a rapid sliding direction reversing happened at the ends of each stroke, and the position records at the end of each stroke were not fully reliable due to the high-speed data acquisition system limitation, and the data for both directions has to be adjusted towards the center of stroke to approach the real position, which created a gap between the red line and the blue line. The adjustment was made according to the difference between wear scar length measurements and data recording system's values.

From the low load (100 N) experimental results in Figure 11, it can be observed that the friction in both directions is mostly symmetrical, except the M test. The reversal friction of negative direction (red solid line) is found to be much lower than that of the positive direction (blue solid line).

Since all the dimples of these three specimens are symmetrical, no directional effect should appear in the friction results. But after checking the wear scar on the M specimen in Figure 10, it is clear that the reversal took place on a row of textures. While for the other two specimens, the reversal was taken place on the land between dimples. Therefore, the first hypothesis is formulated that the textures at reversal point can help building the oil film to reduce the starting friction. Apart from that, the local effect caused by dimples is not clear, and it indicates that a constant lubricant film exists between the roller and the textured specimen under low load.

For high load conditions (right column in Figure 11), the effect caused by dimples are clearly shown, and the dimple affected area (are marked by magenta dashed line) agree with the dimples' positions (gathered from Table 6).

From these figures, it is clearly shown that the step in the leading edge has introduced a friction reduction and the step in the ending edge caused a friction increase. The friction reduction effect at the leading edge is in agreement with the work done by Vladescu [25]. However, since the dimple size of their specimen was smaller than the contact width, no ending edge effect was not observed in

their study. The friction decrease in the leading edge would imply that dimples on the surface work as lubricant reservoirs under high load test conditions. Friction increasing at the ending edge suggests that the micro-hydrodynamic lift from the ending edge may not exist when the dimple size is much larger than the contact width. On the contrary, specific fluid flow may be affected by ending edges, and the film thickness in the ending edge is thinner than that above the dimpled area.
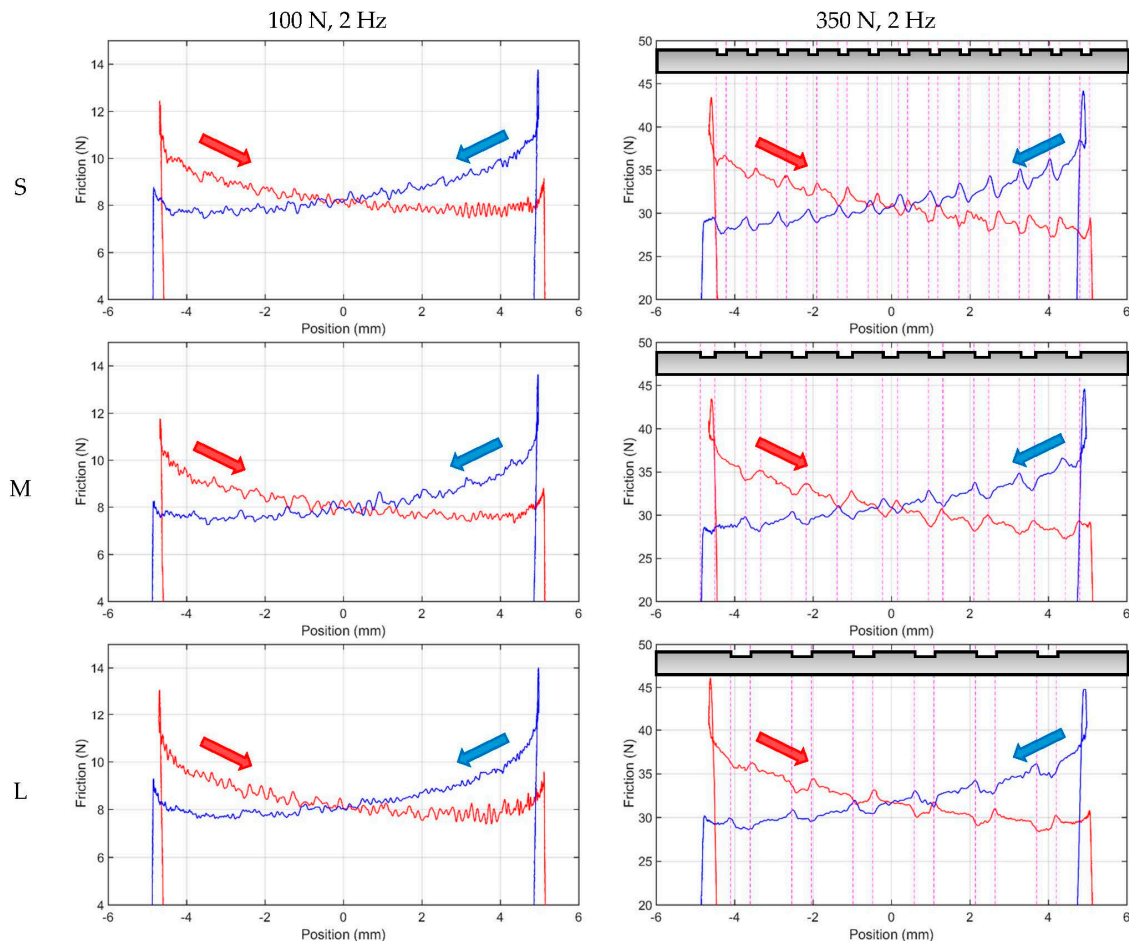
Figure 11. Single stroke friction comparison (100 N, 2 Hz and 350 N, 2 Hz).

To sum up, the overall friction values of textured specimen are lower than smooth surface, and it was thus verified that surface texturing can affect the friction reduction considerably under boundary lubrication conditions.

4. Conclusions

The effect of the square flat bottomed dimple arrays produced by a laser process on the tribological performance of lubricated line-contacts during reciprocating sliding was investigated by measuring the friction coefficient and the topography changes. The conclusions are drawn as follows:

- From the Stribeck curve analysis, all the textured samples have a lower friction coefficient compared to the non-textured samples in the boundary lubrication regime. This effect is attributed to the dimples working as lubricant reservoirs. The lubricant will be squeezed out of the dimple when the roller pressing the dimpled surface, which was called secondary lubrication. This phenomenon happened when solid surfaces were partly in contact.
- Among all the flat bottom dimple tests, no obvious differences were found between dimples with different sizes, which maybe because the contact width is much smaller than the dimple size, and

dimples were not fully covered by the Hertzian contact area. Therefore, the size influence is not obvious under the current test conditions.

- From the low load single stroke analysis, it is observed the friction may decrease when the reversal point locates on the dimples, and it can be deducted that the textures at reversal point can help building the oil film to reduce the starting friction.

- From the single stroke analysis under high load test conditions, the friction decrease in the leading edge indicates that, dimples on the surface work as lubricant reservoirs under high load test conditions. While the friction increasing in the ending edge indicates that, the micro-hydrodynamic lift from the ending edge may not exist when the dimple size is much larger than the contact width. On the contrary, a specific fluid flow may be affected by ending edges, and the film thickness in the ending edge is thinner than that above the dimpled area.

Author Contributions: Ping Lu, Robert J. K. Wood and Ling Wang conceived and designed the experiments; Ping Lu performed the experiments; Ping Lu, Robert J. K. Wood, Ling Wang and Mark G. Gee analyzed the data; Mark G. Gee contributed materials, and Wilhelm Pfleging fabricated the samples; Ping Lu and Wilhelm Pfleging wrote the paper; Robert J. K. Wood, Mark G. Gee and Ling Wang revised the paper.

Conflicts of Interest: The authors declare no conflict of interest.

References

1. Blatter, A.; Maillat, M.; Pimenov, S.M.; Shafeev, G.A.; Simakin, A.V.; Loubnin, E.N. Lubricated sliding performance of laser-patterned sapphire. *Wear* **1999**, *232*, 226–230. [CrossRef]

2. Wang, X.; Kato, K.; Adachi, K.; Aizawa, K. The effect of laser texturing of sic surface on the critical load for the transition of water lubrication mode from hydrodynamic to mixed. *Tribol. Int.* **2001**, *34*, 703–711. [CrossRef]

3. Brizmer, V.; Kligerman, Y.; Etsion, I. A laser surface textured parallel thrust bearing. *Tribol. Trans.* **2003**, *46*, 397–403. [CrossRef]

4. Lu, X.; Khonsari, M.M. An experimental investigation of dimple effect on the stribeck curve of journal bearings. *Tribol. Lett.* **2007**, *27*, 169–176. [CrossRef]

5. Ogihara, H.; Kido, T.; Yamada, H.; Murata, M.; Kobayashi, S. Technology for reducing engine rubbing resistance by means of surface improvement. *Honda R&D Tech. Rev.* **2000**, *12*, 93–98.

6. Bogdan, A. Mechanical seals with sliding surface texture – model fluid flow and some aspects of the laser forming of the texture. *Proc. Eng.* **2012**, *39*, 51–62.

7. Kurella, A.; Dahoptre, N.B. Review paper: Surface modification for bioimplants: The role of laser surface engineering. *J. Biomater. Appl.* **2005**, *20*, 5–50. [CrossRef] [PubMed]

8. Hamilton, D.B.; Walowit, J.A.; Allen, C.M. A theory of lubrication by micro-irregularities. *J. Basic Eng.* **1966**, *88*, 177–185. [CrossRef]

9. Etsion, I.; Halperin, G.; Becker, E. The effect of various surface treatments on piston pin scuffing resistance. *Wear* **2006**, *261*, 785–791. [CrossRef]

10. Wang, X.; Kato, K.; Adachi, K.; Aizawa, K. Loads carrying capacity map for the surface texture design of sic thrust bearing sliding in water. *Tribol. Int.* **2003**, *36*, 189–197. [CrossRef]

11. Qiu, Y.; Khonsari, M.M. Experimental investigation of tribological performance of laser textured stainless steelrings. *Tribol. Int.* **2011**, *44*, 635–644. [CrossRef]

12. Yu, H.; Deng, H.; Huang, W.; Wang, X. The effect of dimple shapes on friction of parallel surfaces. *Proc. Inst. Mech. Eng. J J. Eng. Tribol.* **2011**, *225*, 693–703. [CrossRef]

13. Wang, W.; Huang, Z.; Shen, D.; Kong, L.; Li, S. The effect of triangle-shaped surface textures on the performance of the lubricated point-contacts. *J. Tribol.* **2013**, *135*, 1–11. [CrossRef]

14. Costa, H.L.; Hutchings, I.M. Hydrodynamic lubrication of textured steel surfaces under reciprocating sliding conditions. *Tribol. Int.* **2007**, *40*, 1227–1238. [CrossRef]

15. Vladescu, S.-C.; Olver, A.V.; G.Pegg, I.; Reddyhoff, T. The effects of surface texture in reciprocating contacts - an experimental study. *Tribol. Int.* **2015**, *82*, 28–42. [CrossRef]

16. Shen, C.; Khonsari, M.M. Texture shape optimization for seal-like parallel surfaces: Theory and experiment. *Tribol. Trans.* **2016**. [CrossRef]

17. Hsu, S.M.; Jing, Y.; Hua, D.; Zhang, H. Friction reduction using discrete surface textures: Principle and design. *J. Phys.D Appl. Phys.* **2014**, *47*, 335307. [CrossRef]

18. Yan, D.; Qu, N.; Li, H.; Wang, X. Significance of dimple parameters on the friction of sliding surfaces investigated by orthogonal experiments. *Tribol. Trans.* **2010**, *53*, 703–712. [CrossRef]

19. Mangang, M.; Seifert, H.J.; Pfleging, W. Influence of laser pulse duration on the electrochemical performance of laser structured lifepo4 composite electrodes. *J. Power Sources* **2016**, *304*, 24–32. [CrossRef]

20. Dowson, D.; Higginson, G.R. *Elasto-Hydrodynamic Lubrication: The Fundamentals of Roller and Gear Lubrication*; Pergamon Press: Oxford, UK, 1966.

21. Stachowiak, G.; Batchelor, A.W. *Engineering Tribology*, 4th ed.; Butterworth-Heinemann: Oxford, UK, 2013.

22. Johnason, K.L. *Contact Mechanics*; Cambridge University Press: Cambridge, UK, 1985.

23. Pettersson, U. Surfaces designed for high and low friction. In *Digital Comprehensive Summaries of Uppsala Dissertations from the Faculty of Science and Technology 63*; Acta Universitatis Upsaliensis Uppsala, Uppsala Universitet: Uppsala, Sweden, 2005.

24. Wakuda, M.; Yamauchi, Y.; Kanzaki, S.; Yasuda, Y. Effect of surface texturing on friction reduction between ceramic and steel materials under lubricated sliding contact. *Wear* **2003**, *254*, 356–363. [CrossRef]

25. Vlădescu, S.-C.; Medina, S.; Olver, A.V.; Pegg, I.G.; Reddyhoff, T. The transient friction response of a laser-textured, reciprocating contact to the entrainment of individual pockets. *Tribol. Lett.* **2016**, *62*, 12. [CrossRef]